

## Method to extract difficult-to-evacuate areas by using tsunami evacuation simulation and numerical analysis

Eri Ito<sup>a,\*</sup>, Takato Kosaka<sup>b</sup>, Michinori Hatayama<sup>a</sup>, Luisa Urrea<sup>c</sup>, Erick Mas<sup>c</sup>, Shunichi Koshimura<sup>c</sup>

<sup>a</sup> Disaster Prevention Research Institute, Kyoto University, Gokasho, Uji, Kyoto, 611-0011, Japan

<sup>b</sup> Japan Ministry of Defense, 5-1, Ichigayahonmuracho, Shinjuku, Tokyo, 162-8801, Japan

<sup>c</sup> International Research Institute of Disaster Science, Tohoku University, 468-1, Aoba, Aramaki, Aoba, Sendai, Miyagi, 980-0845, Japan

### ARTICLE INFO

#### Keywords:

Tsunami evacuation plan  
Tsunami inundation simulation  
Agent-based simulation  
Tsunami evacuation facility  
Evacuation difficulty  
Guerrero Gap

### ABSTRACT

Extracting the area where people have difficulty evacuating (hereafter difficult-to-evacuate areas, DEA) when tsunamis hit after an earthquake is important for effective disaster mitigation measures. The DEA was conventionally extracted by simply considering the walking speed, distance to the evacuation destination, and time needed for evacuation after considering the estimated tsunami inundation area. However, evaluating the DEA from such a simple scheme is insufficient because the behavior of residents and the road conditions to the evacuation destinations after an earthquake are not properly reflected in the scheme.

In this study, agent-based tsunami evacuation simulations that can reflect the behavior of residents and real-time changes in the situation were conducted in Zihuatanejo, Guerrero, Mexico. It is a prime sightseeing destination under the high risk of megathrust events in the Guerrero Gap. First, by checking the simulation images at the tsunami arrival time, bottleneck locations were identified, and five additional models with different measures for the bottleneck locations were constructed and tested to find the best model with 195 casualties. Then, focusing on the best model, three indices for the casualties were proposed to extract the DEA effectively and quantitatively, and numerical analyses using the three indices was conducted. Finally, the subdistrict in the center of the target area (subdistrict 5) was quantitatively found to be the district that should be given the highest priority for measures. Moreover, an example model with a new measure in subdistrict 5 was validated to have 101 casualties. The key points for applying the proposed method for extraction of DEA in other areas are summarized.

### 1. Introduction

It is important to extract the area where people have difficulty evacuating (hereafter DEA, difficult-to-evacuate area) from tsunamis after an earthquake and to set appropriate tsunami evacuation facility plans for DEA to ensure more effective disaster mitigation measures. Tsunami evacuation facilities, such as buildings and towers for tsunami evacuation, effectively increase the number of people who get successfully evacuated from the DEA. To the best of our knowledge, the first tsunami evacuation facility in Japan was constructed in 1998, reflecting the 1993 Southwest-off Hokkaido Earthquake. In the 2000s, the newly proposed tsunami damage estimate from the next Nankai Trough Earthquake significantly exceeded the previous estimate; therefore, the Cabinet Office started to designate tsunami evacuation facilities in 2005.

After the 2011 Great East Japan Earthquake, which caused devastating damage in the Tohoku region, related legislations were rapidly enacted, or revised, regarding areas susceptible to tsunami damage across Japan. In light of this trend, studies evaluating the safety of each district using the existing evacuation destination distribution, and evaluating the distribution itself, materialized in the 2000s.

The Ministry of Land, Infrastructure, Transport, and Tourism [1] outlined the following procedure to extract the DEA, which is fundamental information for evacuation destination planning. First, the “time available for evacuation” is calculated by subtracting the “time unavailable for evacuation,” which is the time during which people cannot move because of the earthquake, from the estimated tsunami arrival time after the earthquake occurs. The “maximum evacuation distance” is obtained by multiplying the “time available for evacuation” and the

\* Corresponding author.

E-mail address: [ito@sere.dpri.kyoto-u.ac.jp](mailto:ito@sere.dpri.kyoto-u.ac.jp) (E. Ito).

<https://doi.org/10.1016/j.ijdrr.2021.102486>

Received 29 November 2020; Received in revised form 20 July 2021; Accepted 21 July 2021

Available online 26 July 2021

2212-4209/© 2021 The Authors.

Published by Elsevier Ltd.

This is an open access article under the CC BY-NC-ND license

(<http://creativecommons.org/licenses/by-nc-nd/4.0/>).

walking speed of the evacuees, and the DEA is defined as areas where there is no evacuation destination within the maximum evacuation distance. Minato et al. [2] studied the 1993 Southwest-off Hokkaido Earthquake. The “time unavailable for evacuation” because of the earthquake was derived in detail using the characteristics of the strong ground motion, and the maximum evacuation distances from 112 representative sites were obtained using walking experiments. The DEA was identified by combining this information with the estimated tsunami arrival time, and the validity of the method was evaluated by comparing it with the data recorded. However, people will likely be confused immediately after the occurrence of an earthquake in a real situation. Thus, the evacuation time will be longer than the minimum time necessary for evacuation calculated based on the simple relation between the distance and walking speed or the time necessary for evacuation from walking experiments at normal times. Further, Minato et al. [2] concluded that, based on a comparison of their results with the geological distribution of actual casualties, a “margin” time is necessary in addition to the time required for evacuation based on walking experiments. Results from walking experiments are more realistic than the minimum time necessary for evacuation obtained from geometrical relations, but finding participants with different walking speeds in an experiment is difficult even though there are evacuees with various walking speeds in a real evacuation situation.

Therefore, agent-based simulations that can reflect the behavior of evacuees during the evacuation and the variability in walking speeds would be effective in extracting DEA for planning evacuation destinations.

To evaluate the safety of each district, Minamoto [3] focused on the evacuation process that can only be understood through simulations. They calculated the “tsunami evacuation safety index” of each area from the shape of temporal changes in the evacuation completion ratio and compared the evacuation safety of each district. Osaragi [4] established a simulation model that mirrors existing evacuation plans, and the results were used to calculate detailed evacuation difficulty ratios at the neighborhood level.

Regarding studies that evaluate the existing evacuation destination distribution using simulations, Ohata et al. [5] investigated a city along seaside plains, where evacuation to a land with high elevation is arduous. Further, Takeuchi [6] compared and analyzed cases when the floor area ratio of evacuation destinations was and was not considered. Hamada et al. [7] combined the results of Takeuchi [6] with the results of questionnaires answered by residents to capture the estimated time to start evacuation as well as the direction and destination. Consequently, more realistic simulation parameters were derived. They extracted the DEA by repeatedly conducting simulations in consideration of the evacuation destinations that they newly proposed under conditions from the questionnaires and then evaluated the proposed evacuation destinations. Recently, Ito et al. [8] estimated the strong ground motion wave at the target area considering the characteristics of the underground structure using the knowledge from earthquake engineering, which was then input to a building model for estimating the building collapse rate, and conducted tsunami evaluation simulations considering road blockades from collapsed buildings.

The evaluation of existing evacuation destination distributions outside Japan primarily focuses on Indonesia, which suffered significant tsunami damage from the 2004 Indian Ocean earthquake and tsunami. Specifically, Asher et al. [9] claimed that Padang City, an Indonesian city susceptible to tsunami hazards, has 13 temporary evacuation shelters (TES) but is far from sufficient regarding both capacity and distribution. Therefore, 14 potential TESs (P-TESs) were considered, and buffer analysis of geographic information systems (GIS) was used to investigate how the area where evacuation is possible before tsunami arrival (service area in their terminology) incrementally increased as the number of P-TESs increased from 1 to 14.

To the best of our knowledge, however, several studies estimate the tsunami inundation area (e.g., Santos et al. [10]), the first step for

evacuation planning, we are aware of very few studies evaluating the adequacy of evacuation destinations outside Japan and Indonesia, despite many regions worldwide threatened by tsunamis.

Considering this situation, this study first explores plans to improve evacuation destinations in the central area of Zihuatanejo in Mexico, where there are no guidelines for tsunami evacuation, using agent-based tsunami evacuation simulation methods. Afterward, DEA is extracted under comprehensive judgment using multiple numerical analyzes for understanding evacuation difficulty so that we can effectively draft the improved evacuation destination distribution. Crucial observations from these attempts are reorganized and discussed. This provides a set of standard procedures for developing evacuation destinations from scratch in areas where evacuation destinations have not yet been designated.

## 2. Target area for tsunami evacuation simulations

We chose the central area of Centro in Zihuatanejo as an area for tsunami evacuation simulation, which belongs to Zihuatanejo de Azuta in the Mexican state of Guerrero. This area is called the “Guerrero Gap,” which means there is a high possibility of a big earthquake occurring in the future. Therefore, the study area close to the gap has a possibility of being damaged by an earthquake and the resultant tsunami [11–13]. Fig. 1 shows the location of the target area.

### 2.1. Vulnerability of the target area to an earthquake and tsunami

Low, flat plane below 5 m in altitude spreads from the shoreline to the hills surrounding the target area, which is over 5 m in altitude. The distance between the shoreline and the hill area is approximately 700 m, so it takes about 15 min for adults to move on foot. Such a geological environment makes this area vulnerable to tsunamis caused by earthquakes occurring in the Guerrero Gap.

The target area remains a traditional townscape. Many buildings apart from hotels are two or fewer stories. There are arcades made of wood along streets, and many tourists, who are not familiar with the area, in a tourist season. These characteristics also make evacuation situations more difficult.

The awareness of tsunamis was low in Zihuatanejo before Japanese researchers began to provide disaster education as part of a project in cooperation with Civil Protection [14]. During the field survey in the project, hearings were conducted at the Civil Protection and Department of Tourism, where Japanese researchers demonstrated a trial tsunami evacuation simulation to the staff members. After showing the simulation, one of them mentioned vertical evacuation, which was not included in the trial simulation. Reflecting on the person’s suggestion, Hatayama et al. [15] included a vertical evacuation in the simulation, which means evacuation to hotels. They also performed tsunami evacuation simulations assuming that the residents were assigned as the leading evacuees and solved the problem unique to the tourist spot, which usually hosts tourists unfamiliar with the target area. In the current situation, however, the use of hotels in evacuation situations needs to be explained effectively to hotel owners because they do not readily accept strangers to their hotels because of potential security problems. Therefore, the authority still has a long way to go for planning tsunami evacuation facilities in Zihuatanejo.

### 2.2. Estimation of tsunami inundation area for the tsunami evacuation planning

We also conducted a tsunami inundation simulation of the Pacific coast of Mexico, including the target area. We used the results of the worst-case scenario for the target area in this study as the information used for distributing evacuation destinations in the tsunami evacuation simulation, which will be explained in detail in Section 4.1.1. Here, we explain the process of estimating the tsunami inundation area and its

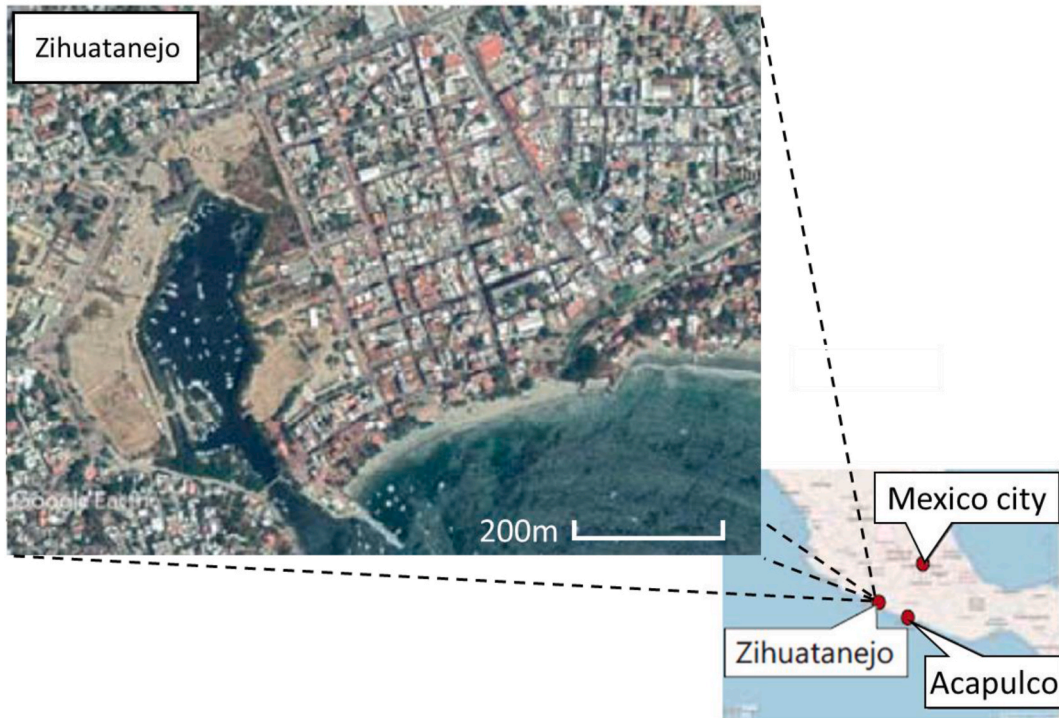


Fig. 1. Location of the target area in this study.

results.

2.2.1. Calculation method and selected scenario

We divided the simulation area into six domains intertwined in a nested grid system (Fig. 2). The details of each domain are presented in

Table 1. In Table 1, cell size refers to the grid size of each domain. Columns and rows are the number of grids in the abscissa and ordinate axes, respectively. The actual width of each domain can be calculated by multiplying the columns and cell size, and the actual length can be calculated by multiplying the row and cell size. XLL and YLL are latitude

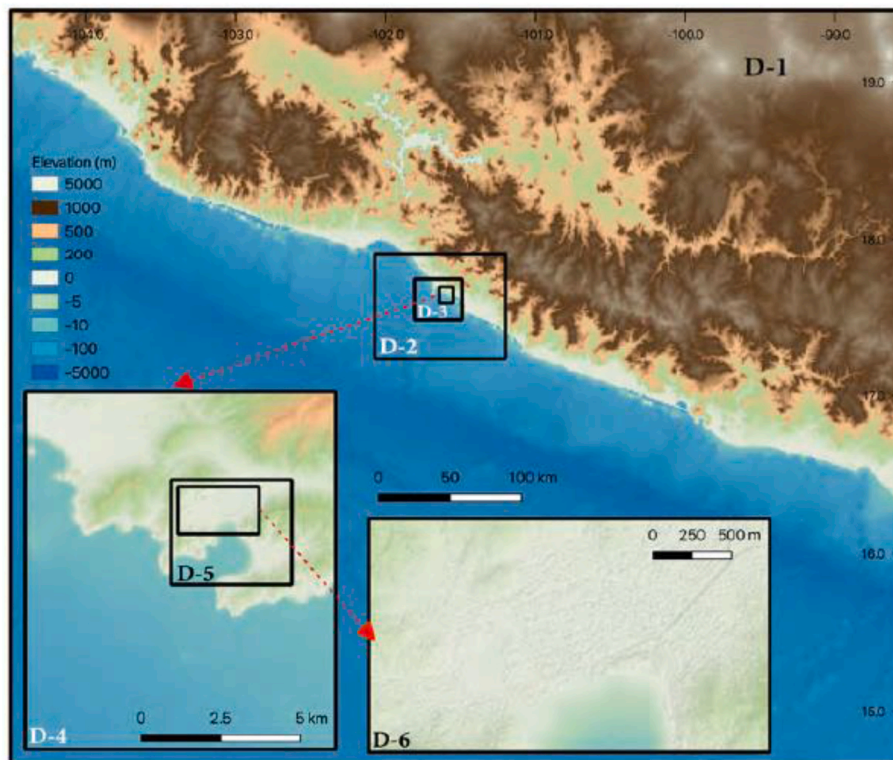


Fig. 2. Computational domains.

**Table 1**  
Computational domains for tsunami numerical simulation.

No.	Cell size (m)	Columns	Rows	XLL (deg.)	YLL (deg.)
D-1	1215	514	436	-104.357393	14.60252
D-2	405	226	184	-102.032973	17.211656
D-3	135	247	214	-101.774215	17.464088
D-4	45	217	250	-101.613167	17.572344
D-5	15	253	220	-101.570617	17.61964
D-6	5	511	298	-101.568843	17.634023

and longitude of the low-left point of each domain in WGS 84 coordinate system. The model used for tsunami propagation and run-up simulation was Tohoku University's numerical analysis model for the investigation of the Near-Field tsunami No. 2 (TUNAMI-N<sub>2</sub>) model [16]. TUNAMI-N<sub>2</sub> is based on nonlinear shallow water equations, which is a two-dimensional approximation of the three-dimensional Navier–Stokes equations for fluid motion.

The tsunami source with maximum tsunami height at 10 m depth offshore Zihuatanejo was selected as the worst-case scenario for detailed simulations in this study. The moment magnitude of the event is Mw 8.35. It was obtained in a probabilistic tsunami hazard analysis conducted by Miyashita et al. [13]; which followed the methods introduced by Mori et al. [17]. In Miyashita et al. [13]; higher resolution data were used to observe the tsunami characteristics in the shallower areas of the bay. Fig. 3 shows the slip distribution of the worst-case for Zihuatanejo. As input for the tsunami numerical modeling, the initial seafloor displacement was calculated using the equations proposed by Okada [18] to solve the surface displacement on rectangular dislocations within an elastic half space.

### 2.2.2. Calculation result

The resultant inland inundation at Zihuatanejo Bay is shown in Fig. 4. The areas with the maximum tsunami inundation depth, nearly 18 m, are “La Madera” beach and “La Ropa” beach, located in the east and southeast of the bay, respectively. Compared to these areas, the

target area for the tsunami evacuation simulation in this study, located in the north in Fig. 4, has a lower tsunami inundation depth but a larger inundation area than these areas because of its low flat plane. In the target area, the horizontal inundation distance was calculated to be approximately 600 m from the coastline to a maximum run-up point of 7.9 m and a maximum of 14 m depth near the coast, which is expected in the worst-case scenario.

As for the tsunami arrival, Fig. 5 shows the tsunami waveform at three reference points (points 1, 2, and 3). Their locations are shown in Fig. 4. The arrival time of the tsunami was not significantly different among the three sites, but the time when the first peak of the tsunami height was reached was different. Point 1 has one peak of the wave height, while two peaks are seen at point 2, and three peaks are seen at point 3. At point 1, the tsunami arrives at 739s after the rupture of the seismic source starts reaching a maximum height of 14 m at 882s. At point 2, the tsunami arrives at 745s after the rupture of the seismic source started and reached the first peak at 812s and the second peak at 893s, respectively. At point 3, the tsunami arrives at 747s after the rupture of the seismic source started and reached the first peak at 811s, the second peak at 861s, and the third peak at 930s. Video1 in supplementary data is a tsunami simulation animation of the worst-case scenario for Zihuatanejo.

We set the distribution of the evacuation destinations in and around the target area by considering the estimated inundation area shown in Fig. 4. The detailed distribution of the evacuation destinations is explained in Section 4.1.1.

## 3. Evaluation system and settings for tsunami evacuation simulations

### 3.1. Evaluation system

The simulation system for this study is composed of a space-time geographic information system (hereafter “GIS”) and a multi-agent simulator (MAS). The GIS was built on “DiMSIS” [19] developed by

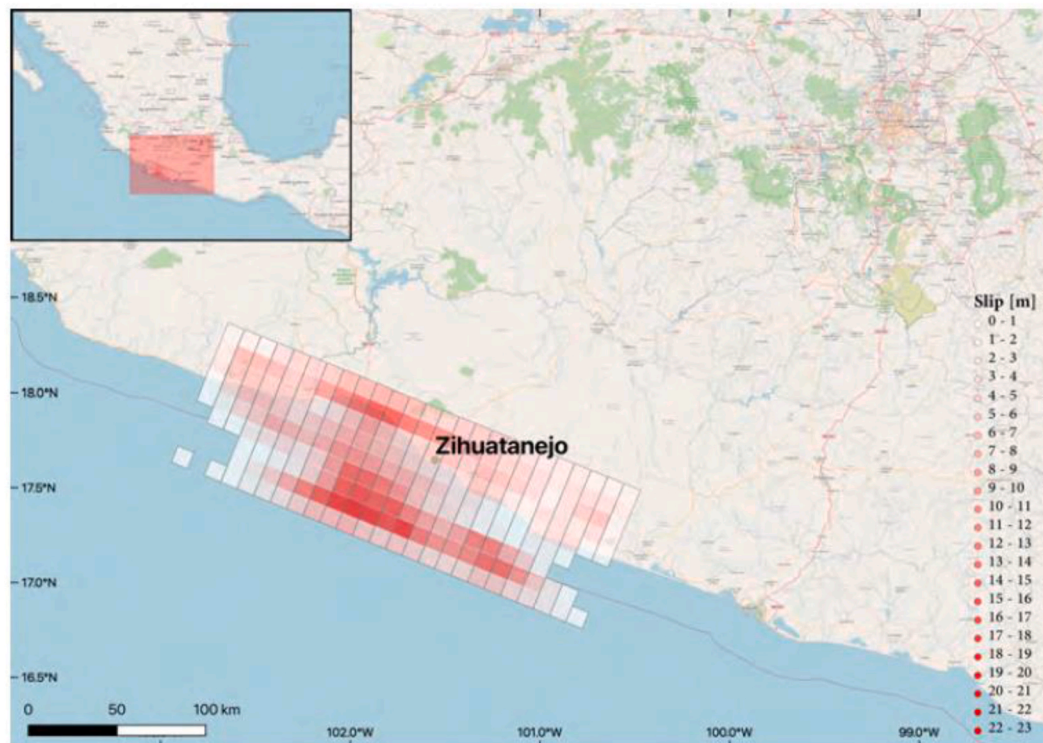


**Fig. 3.** The slip distribution of a Mw 8.35 earthquake offshore Zihuatanejo.

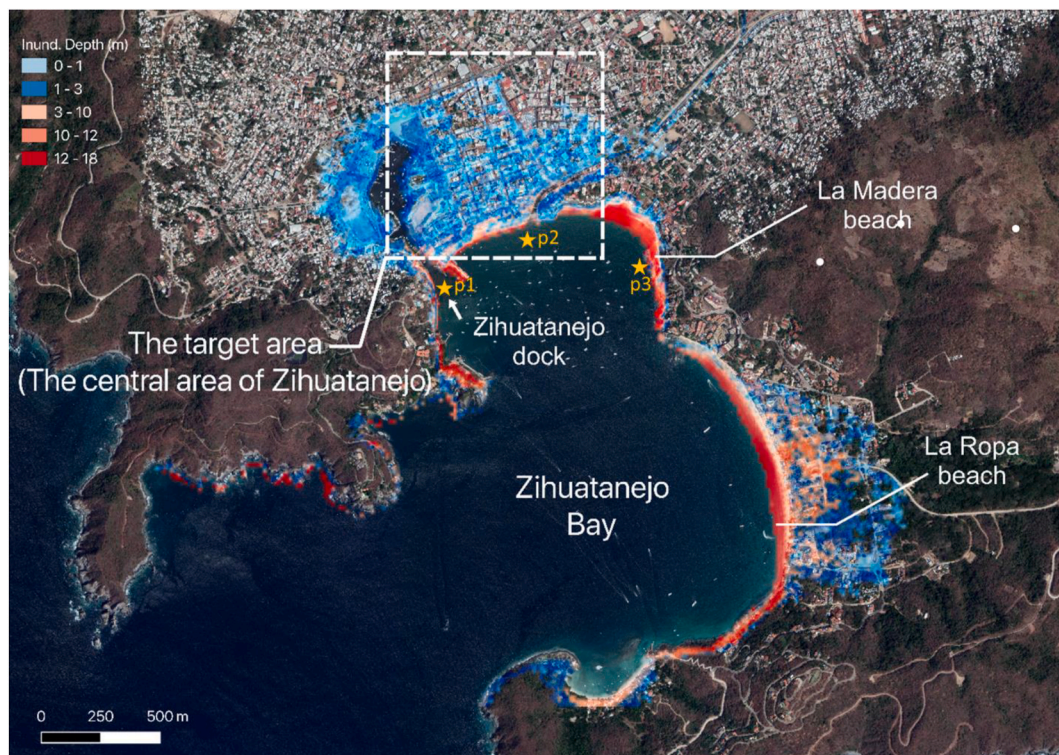


Fig. 4. Maximum inland inundation depth inside the Zihuatanejo bay. The reference points (point1, point2, and point3) for tsunami height variation are also shown as the orange stars (p1, p2, and p3).

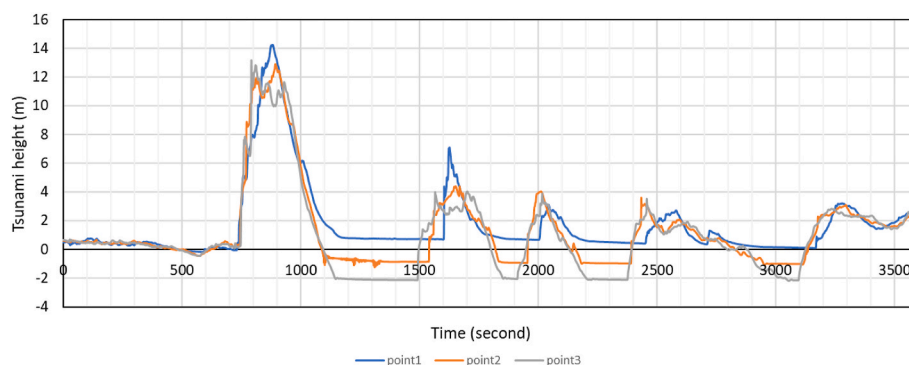


Fig. 5. Tsunami height variation in time history at point1, point2, and point3. The tsunami height is in reference to the mean sea level before the tsunami; thus, a plateau means the moments of tsunami waves receding from the coast.

the Disaster Prevention Research Institute, Kyoto University. The MAS was built on a multi-agent simulation platform, “Artisoc” [20], developed and provided by Kozo Keikaku Engineering Inc.

The source data, including the geographic characteristics and attributes of the residents, the only agents in this simulation, are stored in the database. The positions of the agents at each simulation step are computed on the MAS and returned to the GIS; then, the movements of the agents were evaluated and visualized on the GIS.

As for the data source for the GIS, the road data were acquired from INEGI [21]; and the altitude data were acquired from INEGI [22]. The horizontal resolution of the digital elevation model data was 5 m, and the vertical resolution was 1 m.

To build the data on the GIS, evacuation routes are extracted from the boundary lines acquired from the road and block data from INEGI [21]. Evacuation routes are divided into intersections and road parts. Each intersection has a node number. The direction from the smaller node number to the larger node number is defined as the positive

direction. For road parts, after they are divided into triangles, including the boundary lines on one side, representative points are placed near one side of the triangles. The interval between each representative point was approximately 50 cm. Each representative point has its attribute, which is the angle of the boundary line in the positive direction. This attribute allows agents to move to the next node. The next node to which the agents should go is computed for each road, and agents acquire the next node information at each intersection.

### 3.2. Simulation settings

Here, we introduce the settings for the simulations in this study. The settings are the same as in Hatayama et al. [15]; except for the evacuation destinations.

#### 3.2.1. Environmental settings

In the simulations in this study, road blockades caused by collapsed

buildings were not considered. Some buildings may collapse when a large earthquake occurs, but the possibility that the collapsed building blocks the roads is estimated to be low because almost all the roads are wider than 6 m, and this width is too wide to be blocked by the collapsed buildings.

The time and season when the targeted earthquake occurs is set to be daytime and the high season, respectively. It is expected that the number of victims is the largest during the daytime in the high season because many people, especially tourists, who are not familiar with the area, go out of the buildings or are in the seaside area.

Moreover, the possible evacuation destinations and facilities were considered because they have not yet been designated in the target area. We chose hills over 5 m in altitude and buildings with more than two stories, which corresponds to approximately 5 m because 5 m is estimated to be high and safe enough considering the estimated tsunami inundation height, as shown in Fig. 4. Few buildings have more than two stories, and if any, many of them are not open to the public. Among the taller buildings in the target area, hotels can be considered relatively open to the public because of their business nature. Therefore, in this study, we chose hotels as possible evacuation facilities. The location information of the hotels was obtained from INEGI [23]; and the field survey was conducted in November 2017. We counted the height of each hotel in the field survey and Google Street View. We then chose hotels that were taller than 5 m. As a result, 37 hotels were selected. These hotels are over three stories or two stories with a rooftop floor. Fig. 6 shows the locations of each hotel. After choosing these hotels, we calculated the capacity for evacuees following equation (1):

$$\begin{aligned} \text{Capacity} &= \{(N_f - 2) * A * 0.2\} / S + \{N_r * A * 0.8\} / S \\ &= A / S * \{(N_f - 2) * 0.2 + N_r * 0.8\} \end{aligned} \quad (1)$$

Here, we assumed that the evacuees could enter the hallways, but they could not get into each room. “A” is the projected area of a hotel calculated by QGIS [24] based on an aerial photo from Google Earth, with unit  $m^2$ . If “ $N_f$ ” is the number of stories of the hotel, then “ $N_f - 2$ ” is the number of floors above the second story, of which height is estimated to be sufficient considering the tsunami height. “ $A * 0.2$ ” is the estimated area of the hallways per floor, with  $m^2$  as unit. By referring to the floor map of a hotel in Zihuatanejo, we assumed that the ratio of the hallways to the total floor was 0.2. “ $N_r$ ” refers to the number of rooftop floors. If a hotel has a rooftop floor, then “ $N_r$ ” is 1; otherwise, it is 0. “ $A * 0.8$ ”, with  $m^2$  as unit, is the effective area of the rooftop floors, considering that the edge of the rooftop floor cannot be used as the evacuation space. It would be preferable to calculate the average ratio of the hallways to the total floor and the effective area of the rooftop floors



Fig. 6. Distribution of the hotels (green circles) in the target area.

by investigating the targeted hotels, but because of the security problem, it was difficult to investigate inside the hotels. Therefore, for the ratio of the hallways to the total floor, we adopted the value of a hotel where we could obtain the floor plan, and we estimated the effective area by assuming that 10 % of both ends of one side of the building could not be used as an evacuation space. “S” refers to the effective occupied area per person, of which unit is  $m^2$ /person. The value of S is defined as 1.0 in the tsunami countermeasures promotion manual published by the Fire and Disaster Management Agency in Japan [25].

In the simulation, evacuees basically try to evacuate to a high place. When they find a hotel on their way, they can go there if the hotel’s capacity is not full. Otherwise, they decide to go to the nearest high place.

In this study, we did not consider collapsed hotels, assuming that the old hotels were reinforced to be earthquake-resistant and the new hotels were strong enough to a large earthquake. Considering the real situation in which many buildings collapsed when a big earthquake occurred on September 17, 2017, there is a possibility that some of the hotels that were picked as tsunami evacuation facilities will collapse in the next large earthquake. However, for estimating the damage probability of the hotels, we need to evaluate the vulnerability function of the buildings in Zihuatanejo, which will further take considerable time and effort. Therefore, considering the earthquake resistance of hotels should be a future task for a more realistic tsunami evacuation situation.

### 3.2.2. Parameters for agents

The basic attributes of the people, who are the only agents in the simulations, were configured as follows:

#### I. Population of agents for each attribute

In this simulation, the population was set to 6487, which was estimated from the population data for the daytime. As for the details, according to INEGI [26]; the number of residents is 804. The residents were categorized into three groups according to their ages: 0–7 years old, 8–59 years old, and over 60 years. The number of residents in each category was 587, 117, and 100, respectively. The number of employees working in the targeted area was 3568, which was obtained from INEGI [23]. The seaside area is the tourist area, and according to the municipal officer, the number of tourists in the daytime on weekends was 2000. There is an elementary school in the target area, which is also the main place for disaster education, and it has 100 students.

These numbers may be larger than the actual numbers because there is a possibility that the same person is categorized into more than two categories. However, in this study, we set the total number of people above—6487— as agents in the simulations for the evaluation to be on the safe side.

#### II. Initial position and distribution of agents

Residents are distributed in the buildings in each block by referring to Google Earth, and employees were put in their economic units, which was provided by INEGI [23]. Further, the students were put in their school. As for the tourists, we randomly and manually placed each tourist on GIS, assuming that they are walking around the tourist area which is inside the red square in the right in Fig. 7. The initial positions of agents were each of their neighborhood roads. Fig. 7 shows the initial position of all agents, as well as that of only tourists.

#### III. Direction of evacuation

Every agent has two possible nodes(intersections) that it heads for. The distance from the two nodes to the destination is calculated, and a node that has a shorter distance is defined as the initial direction. In the case where the initial position of an agent is on a dead-end road, the initial direction is the direction to the node connected to another road.



Fig. 7. Location of all agents (left, orange circles) and location of tourists (right, orange circles). Green circles are the hotels designated as evacuation facilities. Tourist area is the area inside the red square.

#### IV. Means of transportation

In this study, we assumed that the agents were educated to evacuate only on foot, and all the people follow what they were educated. It is better to set such a simple constraint for the computation because the primary purpose of the study is not to see the effect of the different parameter settings of the agents but to extract the area where the evacuation may be difficult. In the targeted area, it is expected that using a car for evacuation is not appropriate since they are always parked on either side of many roads, which causes congestion, and there are many one-way roads. It is also expected that abandoned cars will prevent other cars from going through the roads in the evacuation situation, making many people finally give up using their cars. Further consideration of the means of transportation is another future task.

#### V. Walking speed

A walking speed of 0.5 m/s is assumed for residents younger than 7 or older than 60 years, and 1.0 m/s for residents between 8 and 59 years. The walking speed for the employees and tourists is assumed to be 1.0 m/s. There is no survey on the age structure of employees and tourists, but according to the municipal officer, the employees and tourists coming to this area are mainly healthy adults. Each walking speed was based on the guideline for tsunami evacuation plans provided by the Fire and Disaster Management Agency, Japan [25]. We set a walking speed of 0.5 m/s for residents younger than 7 or older than 60 years old, which is the lowest value in FDMA [25]. This is based on a survey on walking speed during the 2011 off the pacific coast of Tohoku earthquake, and by considering the age and health condition of people in Zihuatanejo. The average walking speed during evacuation in the Rias coast area (Kamaishi city), the most severely damaged area in the 2011 off the Pacific coast of Tohoku Earthquake, was an average 0.54 m/s for all ages in a survey conducted by the Urban Affairs Bureau of the Ministry of Land, Infrastructure, Transport and Tourism [27]. The speed is estimated to be even slower for people over 65 years of age. In addition to this estimation, in the target area of this study, there were many people with metabolic syndrome and diabetes who got tired on the way to the destination during an evacuation drill, and their walking was further slowed down because of the slope to the evacuation center. Therefore, the walking speed is expected to be appropriate for the target area. However, in this study, the relationship between walking speed and tsunami flow speed has not yet been examined for the simplicity of the simulation. Bernardini et al. [28] proposed a simulation model that considered flood hydrodynamics and evacuees' motions and

decision-making, while Bernardini et al. [29] showed the walking speed as a function of the floodwater depth through walking experiments in flowing water. The basis of these ideas could be applied to tsunamis, and considering the evacuees' behavior depending on the tsunami depth and water velocity are tasks for more rigorous simulations in future.

#### VI. Basic behaviors of agents and differences depending on awareness of the tsunami risk

In a real situation, it is expected that there will be congestion on the roads while people evacuate. In this study, as the first step in expressing human behavior on congested roads, agents are individually set to avoid obstacles and other agents in front of them. They are set to look around for a step width around themselves and move to diagonally forward directions in the case there is another agent in front of them. If there is another agent diagonally forward, each agent moves to the right and left for a step width and then tries again in the same way. For more realistic human behaviors during the evacuation, we need to consider a more sophisticated simulation model for human behavior, such as that in Ref. [28]. It is based on the source forcing model, which is a dynamics-based model of crowd behavior, and the mutual interference among people and obstacles on the way to the destination can be considered by regarding each person as a particle moving in the plane. As for the path choice, agents take the shortest path. The next node leading to the shortest path to the destination is indicated to the agents when they arrive at each node.

It is also expected that the residents and employees, who are familiar with the area, can choose an appropriate direction for evacuation, whereas the tourists will not know where to go. It is also expected that some of the residents who are highly aware of the vulnerability of the area can evacuate immediately and trigger the evacuation of other people. Reflecting on this situation, Hatayama et al. [15] prepared three categories of agents related to evacuation behavior. In this study, we also categorized the agents into three categories as shown below, based on Hatayama et al. [15].

##### i. Leading evacuees

Leading evacuees are well aware of the vulnerability of the area to the tsunami and can evacuate immediately because they are well prepared for evacuation in advance. They play a role in triggering the evacuation of other evacuees. Their destination after triggering the evacuation of others is the hotel located in the middle of the target area, which is shown as a black star in Fig. 9. There were 17 people among the

residents and employees categorized into this attribute. Hatayama et al. [15] simulated a model in which the number of leading evacuees was 193. After Hatayama et al. [15]; the models with fewer leading evacuees were simulated, and it was found that there was almost no difference in the number of victims between the models with 193 leading evacuees and the one with 17 leading evacuees, if the leading evacuees were placed on all the roads appropriately in the targeted area. In other words, 17 is the minimum and most effective number of leading evacuees for reducing the number of victims. Since we are planning to ask the residents for their cooperation in becoming the leading evacuees, this can be a feasible number for cooperation. In this study, we performed simulations under the assumption that the 17 residents were assigned to be leading evacuees by mutual agreement, and were well prepared for the evacuation.

#### ii. Basic evacuees

Basic evacuees are familiar with the area but are not aware of the tsunami risk. Therefore, they need more time to prepare for evacuation than leading evacuees. They start to evacuate 5 min after the earthquake stops. Residents and employees, except for those assigned to be the leading evacuees, are categorized into this attribute. Basic evacuees initially have the destinations, which are the intersections in the hill, which will be explained in detail in Section 4.1.1. When they find a hotel on the way, they change the destination from the intersection in the hill to the hotel until it reaches its capacity. If there are multiple hotels on the same road, they can choose the nearest one. After the hotel reaches its capacity, they can no longer evacuate to the hotel.

#### iii. Following evacuees

Following evacuees are those who do not know the appropriate destination or evacuation route. Tourists are categorized into this attribute. They cannot start evacuating without seeing other evacuees moving and evacuate when they see the others do so within 15 m from them.

They do not react to the other evacuees in different links or on different nodes, even if they see the other evacuees within 15 m. They acquire the destination node number from the agent they are following. When they have already started, they also acquire the destination hotel of the other agent they are following. When the hotel reaches its capacity, they cannot evacuate, which is the same as basic evacuees.

### VII. Starting time to evacuate

We assumed that the time for which evacuees are unable to move due to the earthquake was 1.5 min, based on the experience from the Great East Japan Earthquake that occurred in 2011. We set the start time of the simulation at 1.5 min after the earthquake. The starting time to evacuate differs depending on the attributes of the evacuees mentioned above. Leading evacuees start to evacuate at the start time of the simulation, while basic evacuees start 5 min after the start time of the simulation. Following evacuees start after they see other agents evacuating. Fig. 8 shows the time to start the evacuation for all evacuees.

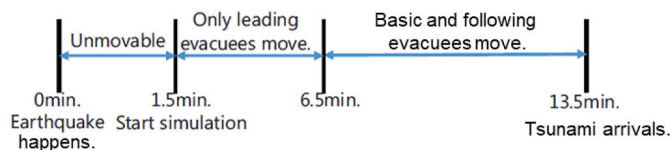


Fig. 8. Time to start evacuation for all the evacuees. The start time of the simulation is set to 1.5 min after the earthquake happens.

## 4. Extraction of the DEAs by using agent-based tsunami evacuation simulation

### 4.1. Two-step method for extracting the DEAs and results

#### 4.1.1. Construction of the new models by focusing on the bottleneck locations of the simulation image at the tsunami arrival time (step 1)

Tsunami evacuation simulations were conducted using the parameters described above. We first drafted the initial model; then, two series of models, A and B, were drafted by considering the bottleneck locations in the simulation image at the tsunami arrival time and whether actual implementation is possible. Each model was simulated for three trials, and the number of casualties in this study was the average of three trials. The difference in casualties within each model was significant, as explained below. In ad-hoc searching, as is employed in this study, the evaluation and comparison of many models through trial and error is more important than obtaining highly converged results in each model. Thus, simulation for three trials is sufficient at this stage.

The definition of “casualties” in this study is the number of evacuees that could not complete the evacuation to the intended destination within 12 min after the start of a simulation by considering the estimated tsunami arrival time of 13.5 min, which was explained in Section 2.2.2, and the unmovable time of 1.5 min, which was explained in Section 3.2.2. If temporal simulated tsunami data are available, a more accurate evaluation of whether evacuation for each agent could be successfully completed by overlapping the temporal tsunami data with the position of evacuees at each moment on a GIS. However, such data were not available in this study so that we cannot help but make such simulation a future task.

#### I. Initial model

In the initial model, hotels, hills that surround and spread to the east and north of the target area, and a bridge adjacent to the sea to the southwest of the target area are designated as tsunami evacuation destinations. Fig. 9(A) shows the locations of evacuation destinations. Hotels are indicated by green circles, and the node number adjacent to a hill is indicated by red letters. The area near the node numbers in the east and north is higher than 5 m in altitude; therefore, it is not included in the tsunami inundation area. Node number 2 in the southwest is where there is a bridge connected to a hill. Hills could be reached just after crossing this bridge; hence, the node number near this bridge is considered as an evacuation destination. Fig. 10(A) shows the distribution of evacuees 12 min after the start of the simulation. The total number of casualties was 2326. As is evident in the Figure, many casualties are found heading to the hills in the east and via the bridge to the south.

#### II. A-1 model

In the A-1 model, additional evacuation measures in the main avenue in front of the eastern hills are taken apart from the hotels in the initial model. This is because many casualties in the initial model were evacuees who evacuated to the eastern hills. Fig. 9(B) shows all evacuation destinations in the A-1 model. The node numbers in the red-filled boxes are evacuation destinations newly added to the A-1 model. As for implementing the additional evacuation measure, there are a few options, and in reality, the evacuation measure with the best cost performance will be selected after cost evaluation. In this study, we only designated locations with the evacuation measure and did not set a specific measure. The number of casualties was 549; thus, many lives were saved compared to the initial model. However, there are casualties in front of the main avenue, and is a congestion at the southern bridge. Therefore, a model to save these people was drafted in the next A-2 model. Fig. 10(B) shows the casualty distribution.

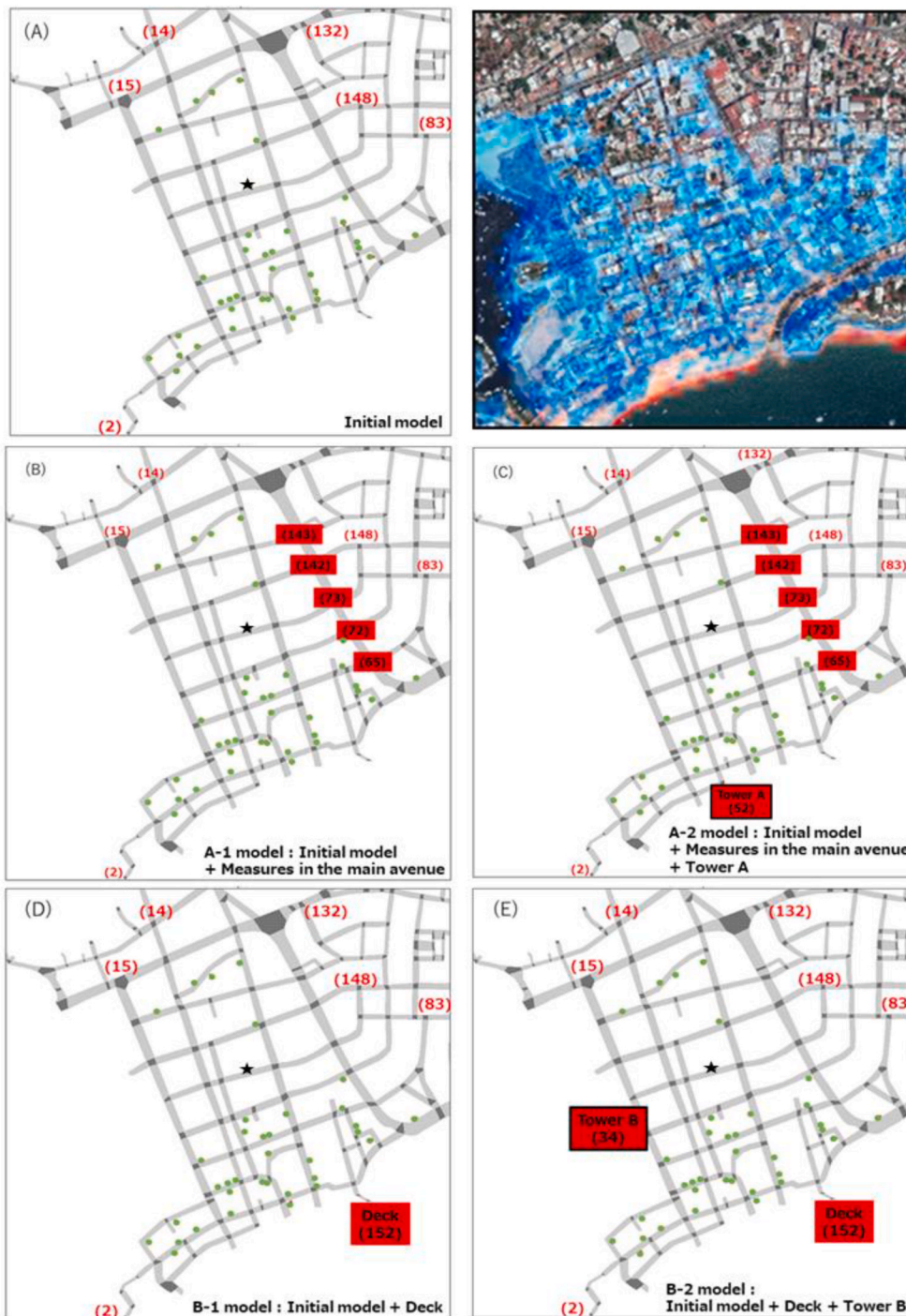


Fig. 9. Estimated inundation area (top right) and evacuation destination distribution of each model. The green circles and a black star indicate hotels. A hotel shown in black star is the one the leading evacuee evacuate. The numbers in brackets are the node number adjacent to hills that are used as evacuation destinations. The initial, A-1, A-2, B-1, and B-2 models are shown as (A), (B), (C), (D), and (E), respectively. The node numbers of evacuation destinations newly added in the A-1 and B-1 models are shown in red-filled boxes, while those of the evacuation destinations newly added in the A-2 and B-2 models are shown in a black rectangular frame (Tower A and B, respectively).

### III. A-2 model

In the A-2 model, a tsunami evacuation tower A is set to be constructed in addition to the hotels, hills, and main avenue measures in the A-1 model. Fig. 9(C) shows all evacuation destinations in the A-2 model. The location of the newly added evacuation tower is shown as a black rectangular frame. The casualties at the southern bridge in the A-1 model evacuated to a relatively longer distance compared to other evacuees. Therefore, tsunami evacuation tower A was set to be located at the center of the seaside area (node number 52), which has vacant space and is easier to access than the southwestern bridge at node number 2. The total number of casualties was 195. There was a decrease in the number of evacuees who failed to evacuate because of the congestion

while evacuating to the bridge south of node number 2. Contrarily, there are still casualties in front of the eastern main avenue. Fig. 10(C) shows the casualty distribution.

### IV. B-1 model

In the B-1 model, in addition to the hotels and hills, a pier to the southeast of this area, which connects to land with elevations higher than the inundation height, is considered as an evacuation destination. This reflects the result where many casualties tried to evacuate to the eastern hills in the initial model. Fig. 9(D) shows all the evacuation destinations. The pier newly added as an evacuation destination, which leads to higher land, is located at node number 152. The node number is

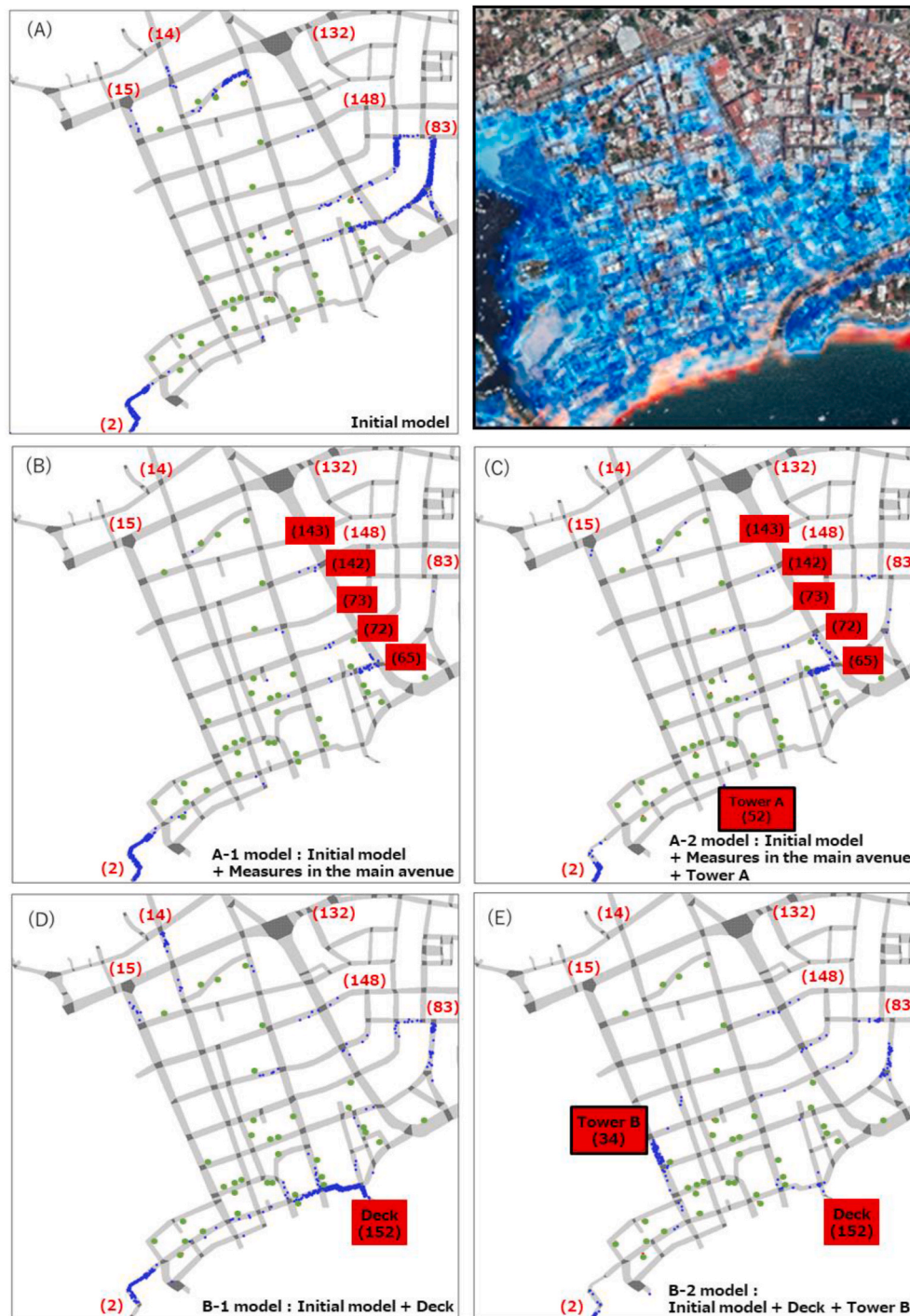


Fig. 10. Casualty distribution at the tsunami arrival time in each case (one example out of three trials). The green circles are hotels designated as tsunami evacuation facilities, and the blue circles are failed evacuees.

considered as a goal in this model. There were 645 casualties, and the main reason why the evacuees failed to evacuate is the congestion on the roads leading to the pier. Moreover, the congestion near node number 2, which is the southwestern bridge, was not resolved. Fig. 10(D) shows the casualty distribution. The next model aims to save these people.

V. B-2 model

In the B-2 model, tsunami evacuation tower B is set to be constructed at a location where hotels, hills, and a pier to higher land cannot sufficiently accommodate evacuees. Fig. 9(E) shows the evacuation

destinations in the B-2 model. The added tsunami evacuation tower B was set to be located close to node number 34. Fig. 9(E) shows the location with a black rectangular frame. The reason for adding tsunami evacuation tower B at node number 34 is as follows. By tracking the motion of people stuck in congestion at the pier in the B-1 model, it was found that evacuees that were relatively distant from the pier failed to evacuate. Therefore, a tsunami evacuation tower near the yacht harbor in the western main avenue was added as an evacuation destination. The total number of casualties was 181. The congestion at the pier at node number 152 and the southern bridge at node number 2 were significantly mitigated. However, there were casualties near tsunami

evacuation tower B, which was newly added near node number 34, and around the eastern hills. Fig. 10(E) shows the casualty distribution.

In the A-2 and B-2 models, a tsunami evacuation tower was set to be constructed at an appropriate location because it is feasible with the support of city officials and residents. The capacity of the hills is estimated to be sufficiently larger than the number of people in the target area; therefore, it was not explicitly considered. After performing the simulations, it was found that Tower A and Tower B accommodated 473 evacuees and 448 evacuees on average in 3 trials, respectively. Considering that there is a tsunami evacuation tower that accommodates up to 600 evacuees in Japan, these numbers of evacuees accommodated into towers A and B are feasible. As mentioned above, the capacities for evacuation destinations other than hotels were not considered, but there was no significant effect on the results. This is because the results from several repeated simulations revealed that evacuees who evacuate to destinations other than hotels fail because of the evacuation time rather than the capacity of the tsunami evacuation destinations. Contrarily, the evacuation time is not the decisive factor for hotels because they are located inside the target area and are accessible within 12 min after the start of the simulation. Instead, capacity is a more decisive factor and must be considered.

#### 4.1.2. DEA extraction in the best model of step 1 by numerical analysis with three indices (step 2)

The number of casualties decreased to less than 200 in both the A-2 and B-2 models due to the improvement in 2 steps from more than 1200 in the initial model. A comprehensive combination of these models can yield the best model. However, constructing two evacuation towers is unrealistic when construction costs are considered. In addition, it is not economical because the number of casualties in models A-2 and B-2, where the first tower is constructed, is already small compared to the total population of the target area. Rather, it would be wise to first analyze in detail the best model among the models drafted so far and extract the district that does not benefit from the measures in the best model, then focus on and take measures on such a district. In addition, there is no doubt that the ultimate goal of a disaster mitigation plan is to save every life, and having a model with as few casualties as possible is important to motivate city officials and residents to participate in evacuation drills.

Therefore, to further improve the model with minimum cost, by using the A-2 model, which is more feasible and has fewer casualties and is considered as the best model, numerical analyses with three indices for evaluating the evacuation difficulty were adopted to grasp the current movement patterns of evacuees and to comprehensively extract the DEA.

Before the analyses, the A-2 model was first simulated for 10 trials to obtain more stable results, and the initial position of the casualties in each simulation was obtained. Fig. 11 shows the initial positions of the casualties in the first trial.

To extract the issues in more detail, the target area was separated into nine subdistricts based on the obtained initial position distribution of the casualties. Fig. 12 shows the splitting into subdistricts, and Table 2 shows the total population of each subdistrict.

After these preparations, as the first analysis, the total number of casualties was obtained, which is the fundamental information for evaluating the evacuation difficulty of a subdistrict. Next, the ratio of casualties to the population in each subdistrict was calculated as the second analysis. Evaluating only by the absolute number alone is not sufficient because it picks up only the area with the largest number of casualties. Therefore, the relative number, which is the ratio of the casualties to the total number of evacuees in the subdistrict, is required for an appropriate evaluation. By using the relative number, we can extract the area where there is a high possibility for evacuees to fail to evacuate; in other words, the area where a measure would effectively reduce the casualties. However, using only the relative number is insufficient because it may not pick the area with the largest number of casualties.



Fig. 11. Initial position of casualties in the first trial of the A-2 model. Blue circles show the initial position of the casualties while orange circles show the location of the initial position of all the people. Green circles are the hotels designated as evacuation facilities.

Evaluation using both absolute and relative numbers makes the evaluation more comprehensive. Fig. 13 shows the number of casualties in each subdistrict. The ordinate is the average number of casualties from 10 trials, and the abscissa is the subdistrict number. Fig. 14 shows the ratio of casualties to the total population in each subdistrict. The ordinate is the ratio obtained by dividing the number of casualties, which is the average number for 10 trials in Fig. 13, by the population of the subdistrict in Table 2. The abscissa represents the number of subdistricts.

Further, to understand the behavior of each casualty in detail, as the third analysis, the number of failed evacuations among the 10 simulations was calculated for an agent, and the number of agents that failed simultaneously was counted in each subdistrict. The goal of this analysis is to observe the “chance of becoming a casualty” of each agent, which can explain why evacuation is hampered in this subdistrict. This information is valuable when drafting improvement plans. In subdistricts where many agents fail to evacuate in almost all the 10 trials, a possible reason for failed evacuations is that the distance to an evacuation destination is too long for the agents. In contrast, in subdistricts where there is scattering in the number of agents that failed to evacuate for a certain number of times among 10 trials, there may be several reasons that hamper evacuation in the subdistrict instead of a single cause such as “distance.” For the former subdistrict, a single measure enacted in the subdistrict would effectively reduce casualties. For the latter, taking relatively low-cost measures in multiple locations could be more appropriate than one intensive measure.

The results of this analysis are shown in Fig. 15. In this study, most of the failed agents failed all 10 times in subdistricts 5 and 2, while the number of failures of agents in subdistricts 1 and 4 were scattered.

Finally, the evacuation difficulty of subdistricts was comprehensively evaluated based on the above three analyses. Subdistricts 5 and 1 have consistently significant evacuation difficulties, as shown in Figs. 13–15. Subdistrict 5 has more agents that fail compared to subdistrict 1; thus, investment in subdistrict 5 has a higher priority for taking a pinpointed measure. Subdistrict 5 is located in the center of the district, far from each evacuation site, and is intuitively considered to be a difficult place to evacuate, but intuitive judgment cannot be a

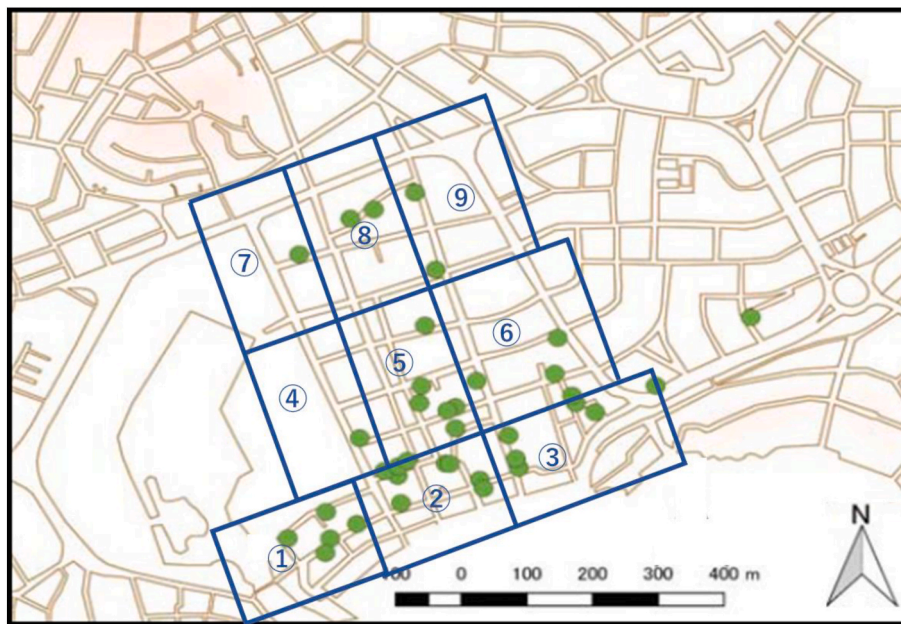


Fig. 12. Splitting of the target area. The boundary of each subdistrict is shown by blue lines, and the number within the blue boxes is the subdistrict number. Green circles indicate the locations of the hotels designated as evacuation destinations.

Table 2  
The total population of each subdistrict.

Subdistrict number	1	2	3	4	5	6	7	8	9
Number of people	926	1169	1144	265	441	1266	230	405	641

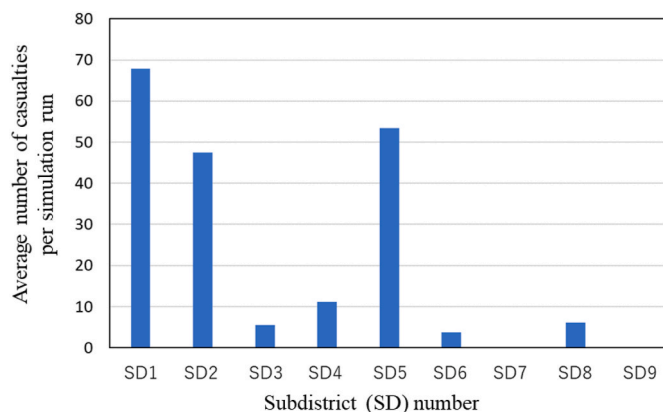


Fig. 13. Average number of casualties per run in each subdistrict. SD in the abscissa stands for subdistrict.

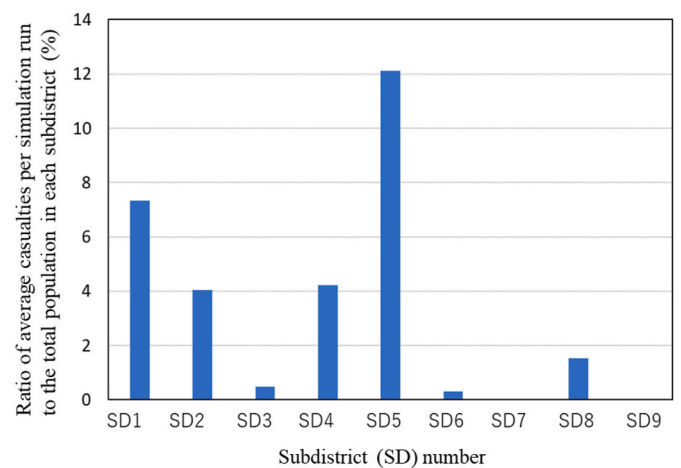


Fig. 14. Ratio of average casualties per simulation run in Fig. 13 to the total population in each subdistrict.

motivation of the stakeholders to take concrete measures. The proposed method was able to quantitatively demonstrate it.

4.2. Points of the proposed method for application to other areas

Here, we provide a few key points to apply the proposed method to areas other than the target area in this study after the detailed explanations are added to the following two procedures.

First, in step 2, before the three types of analysis, the A-2 model was simulated for 10 trials because the results from our MAS were found to sufficiently stabilize after 10 trials. The number of trials depends on the number of people in the district, the complexity of the conditions, and the randomness of the simulator. Therefore, confirming the stability of the results is important when applying this method to different cases.

Second, the area was divided into nine subdistricts based on the initial positions of the casualties to make the differences between each subdistrict more apparent. If the district can be physically divided by geographical features, this division can be used instead of the proposed method. Division by administrative district is an option if the size is appropriate. Dividing into subdistricts with a similar number of evacuees is another possible method, although we still need to decide arbitrarily to draw lines between subdistricts.

To summarize, the proposed method in this study and a few key points in the case of applying the method to other areas are as follows:

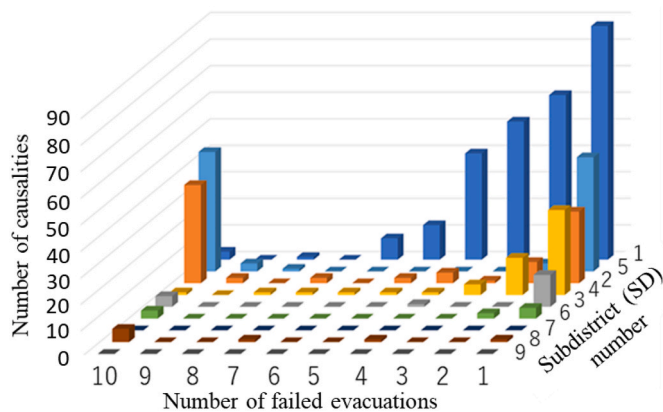


**Fig. 15.** The distribution of the number of failures for agents that become casualties in each subdistrict. The y-axis axis is the subdistrict number. The x-axis is the number of failed evacuations among 10 trials for an agent, and the z-axis is the number of agents with the same number of failures. In other words, the number of a bar shows the number of agents, where the initial position is in the corresponding subdistrict, that fail for the number of times in the x-axis among 10 trials. Different agents become casualties in subdistrict 1, while the same agent repeatedly fails in different trials and there are many such agents in subdistricts 5 and 2.

- I. Draft the improved simulation models reflected the findings from the simulation images at the tsunami arrival time. Various models considering feasibility should be drafted with a minimum number of trials in the simulation after validating the randomness of the simulator.
- II. Choose the best model among the improved models and perform simulations. Additional trials in new simulations are needed until the results converge to obtain more accurate results.
- III. Divide the target area into subdistricts. Possible dividing methods are a) dividing by seeing the distribution of casualties, b) dividing into subdistricts with a similar number of evacuees, c) dividing by the geological features, and d) dividing by the administrative district.
- IV. Perform three types of numerical analyses to understand the evacuation difficulty in each subdistrict and extract the DEA among the subdistricts by comprehensively considering the results from the analyses.
- V. Propose an appropriate measure of the DEA considering the feasibility and financial situation in the target area. Tangible and intangible measures can be considered depending on the situation in the target area.

4.3. Discussion

One significant feature of this study is to extract the DEA not by using the simple relation between the distance to the evacuation destination, the time needed for evacuation, and walking speed, but by conducting simulations using MAS that can reflect the congestion of the road and the behavior of the agents. By adopting this simulation to extract the DEA, we can grasp a more realistic situation of the casualties and then take appropriate measures based on the results. To recognize the difference between the two methods mentioned above, we first categorized the casualties in the A-2 model using the time needed for evacuation calculated by the simple relation between the distance to the evacuation destination and walking speed, which is the basic idea often used for extracting DEAs, as shown in the abstract. Here, we call the time needed for evacuation, calculated above, as “simply estimated evacuation time.” Then, we compared the simply estimated evacuation time with the estimated tsunami arrival time (12 min after the start of the simulation), and checked if there were any casualties with the simply estimated evacuation time that was less than 12 min. Fig. 16 shows the distribution

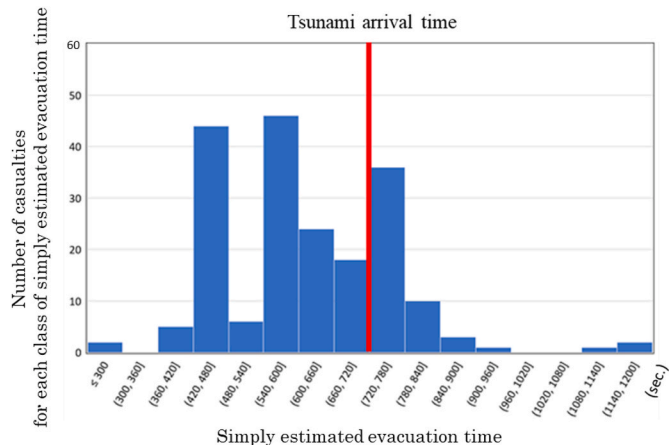


**Fig. 16.** Distribution of the number of casualties categorized by each simply estimated evacuation time with an interval of 120 s. The abscissa is the simply estimated evacuation time. The ordinate is the number of casualties for each class of simply estimated evacuation time. Bins give the number of casualties computed by the agent-based simulation for each class of simply estimated evacuation time. Those with simply estimated evacuation time earlier than 12 min are regarded as safe when applying the simply estimated evacuation time calculation method. The estimated tsunami arrival time, 12 min (720 s), is also shown on the Figure. All the time is counted from the starting time of the simulation.

of the number of casualties by simulation for each class of simply estimated evacuation time. In Fig. 16, the estimated tsunami arrival time, 12 min, is also shown to be compared with the simply estimated evacuation time. The number of casualties comes from the result in the third run of the simulations among 10 trials; here, we show this Figure as an example of 10 trials. Fig. 16 shows that the simply estimated evacuation time for a considerable number of casualties is less than 12 min. This means that they are estimated to evacuate successfully in the case of the evaluation by the evacuation time from the simple relation between the distance to the destination and walking speed. Therefore, we can say that the result of the casualties from the simulation is evaluated on the safe side.

Another important feature of this study is that we extracted the DEA using three types of numerical analyses to understand the evacuation difficulty. From these analyses, subdistrict 5 was evaluated as a district where priority measures should be taken. Reflecting on the evaluation above, we simulated a new model with an additional tsunami evacuation facility as an example to verify the evaluation of the proposed method. In subdistrict 5, there is a municipal tax office with three stories and a roof floor. It was constructed relatively recently and had sufficient floor space. The municipal tax office is a public building, so it would be easier to be designated as a tsunami evacuation facility with the cooperation of the authorities than hotels, of which owners do not want to let strangers enter because of potential security problems. Therefore, in the new simulation model, we designated this building as an additional tsunami evacuation facility. The other evacuation destinations follow the A-2 model. Fig. 17 shows the distribution of the evacuation destinations in the new simulation model.

Before conducting the simulation, the floor space of the municipal tax office was estimated based on a satellite image, and the capacity was calculated to be 553 people based on equation (1) to calculate the hotel capacity shown in Section 3.2.1. Then, simulations of the new model were conducted for 10 trials. Fig. 18 shows a comparison of the average number of casualties in the new model with the A-2 model from ten trials. The average number of casualties in the entire target area was 101, approximately half of that in the A-2 model (195), as shown in Section 4.1.1. Focusing on the result in each subdistrict, in subdistrict 5, the number of casualties was 9, while it was 53 in the A-2 model, which

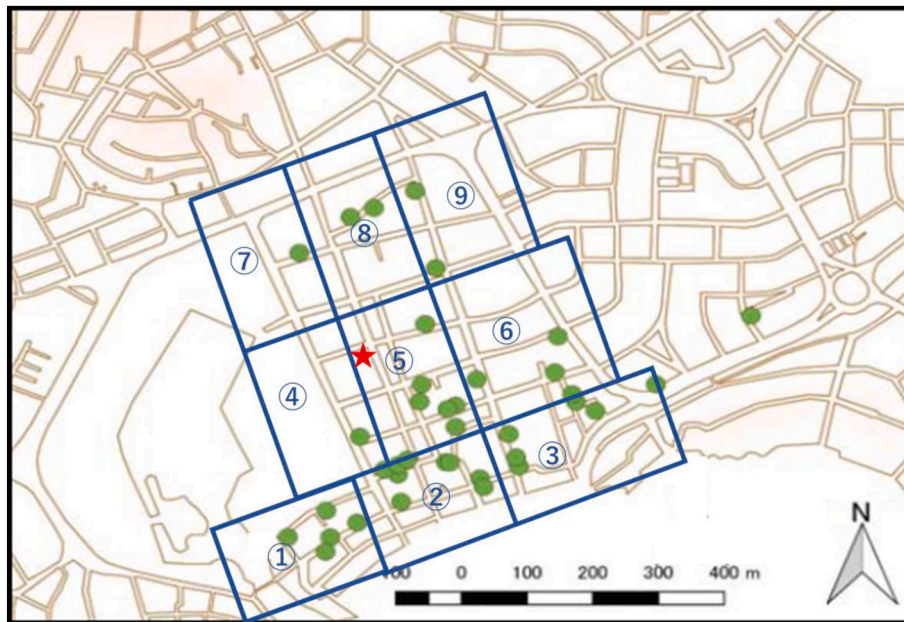


Fig. 17. Location of the municipal tax office newly considered as a tsunami evacuation facility (red star symbol). Green circles are hotels that were designated as tsunami evacuation facilities from the initial model. The boundary of each subdistrict is shown in blue lines, and the number within the blue boxes is the subdistrict number.

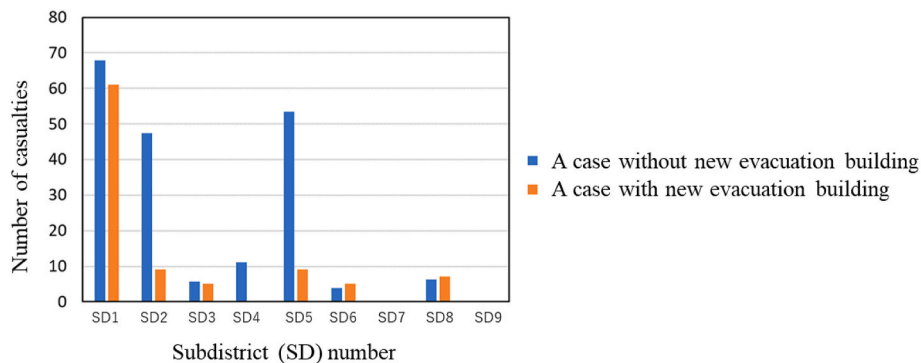


Fig. 18. Comparison of the average number of casualties in each subdistrict from 10 trials of the A-2 model and the model where the tsunami evacuation facility in Fig. 17 is newly added.

corresponded to 2 % and 12.1 % of the total number in the district, respectively. Positive effects were also found in subdistricts 2 and 4. This result shows that the evaluation of the three types of numerical analyses for understanding the evacuation difficulty is reasonable.

### 5. Conclusion

This study conducted tsunami evacuation simulations to extract the DEA (difficult-to-evacuate area) from a tsunami in Zihuatanejo, Mexico, where there is insufficient awareness of evacuation among residents, and administrative agencies are still investigating evacuation plans.

In step 1, the initial model was drafted, and the location of casualties at the estimated tsunami arrival time was captured using the simulation images, and improved models were drafted by repeatedly adding feasible evacuation destinations. In the end, we had 195 expected casualties in the A-2 model, which was considered the best model among the drafted models.

In step 2, detailed analyses were performed using the A-2 model. The target area was divided into nine subdistricts, and three numerical analyses were performed to understand the evacuation difficulty of each subdistrict. The evacuation difficulty of each subdistrict was

comprehensively evaluated, and the DEAs were extracted from the three indices on the casualty, namely, the absolute number, relative number, and distribution of the number of failures for each agent. Subdistrict 5, the central district in the target area, was found to be the district where a priority measure should be taken. Moreover, a few key points of the proposed method to extract the DEAs were provided for their application to other areas.

In the discussion, focusing on the casualty in the A-2 model, simply estimated evacuation time, calculated by dividing the distance to the destination by the walking speed, was calculated, and its relation with the number of casualties obtained by our simulation was checked. It was found that a considerable number of evacuees with simply estimated evacuation time of less than 12 min failed to evacuate in our simulation. This means that the simply estimated evacuation time is evaluated on the dangerous side.

Based on the results of step 2, subdistrict 5 was a priority area for taking measures. The new model in which the municipal tax office in subdistrict 5 was used as a tsunami evacuation facility was simulated. The ratio of casualties to the population in subdistrict 5 decreased from 12 % in the A-2 model to 2 % in the new model, whereas the ratio to the total population in the target area, 6487, decreased from 3 % in the A-2

model to 1.5 % in the new model.

As for the future tasks, we first need to verify the three other ways to divide the target area into smaller subdistricts summarized in Section 4.2, namely, dividing into subdistricts with similar numbers of evacuees, dividing by the geological features, and dividing by the administrative district.

This study targeted an area with an intermediate size, a population of approximately 6000 people and an area of approximately 0.4 km<sup>2</sup>. We wish to evaluate whether the proposed method for extracting DEA is effective in tsunami evacuation simulations of districts with larger populations and areas.

## Funding

This research was supported by the Science and Technology Research Partnership for Sustainable Development project, “The Project for Hazard Assessment of Large Earthquakes and Tsunamis in the Mexican Pacific Coast for Disaster Mitigation” (JPMJSA1510).

## Declaration of competing interest

The authors declare that they have no known competing financial interests or personal relationships that could have appeared to influence the work reported in this paper.

## Acknowledgment

We thank Prof. Nobuhito Mori from Kyoto University for providing the tsunami source used in the tsunami simulation. The bathymetric and topographic data for the worst-case scenario simulation were kindly provided by the Department of Atmospheric Sciences of the National Autonomous University of Mexico (Special thanks to Dr. Jorge Zavala Hidalgo).

## Appendix A. Supplementary data

Supplementary data to this article can be found online at <https://doi.org/10.1016/j.ijdr.2021.102486>.

## References

- [1] Ministry of Land, Infrastructure, Transport, and Tourism (MLIT), A guideline for community planning for tsunami disaster mitigation [in Japanese], <https://www.mlit.go.jp/common/001000488.pdf>, 2013.
- [2] F. Minato, Y. Hata, T. Nakashima, M. Koyama, Y. Kuwata, M. Yamada, K. Tokida, Evaluation of difficult area for tsunami evacuation in Aonae district Okushiri Island, Japan, based on strong ground motion estimation and walking experiment during the 1993 Southwest Hokkaido earthquake, *J. Jpn. Soc. Civ. Eng. Ser. B3 (Ocean Eng.)* 72 (2) (2016) I\_509–I\_514 [in Japanese].
- [3] T. Minamoto, Y. Nariyuki, Y. Fujiwara, A. Mikami, Development of tsunami evacuation simulation system and its application to assessment of area refuge safety, *J. Jpn. Soc. Civ. Eng. Ser. A1 (Struct. Eng. Earthquake Eng.)* 65 (1) (2009) 757–767 [in Japanese].
- [4] T. Osaragi, T. Oki, Difficulty of evacuation in densely built-up area in the aftermath of a large-scale earthquake, *J. Architect. Plann., ALJ* 77 (68) (2012) 2561–2567 [in Japanese].
- [5] D. Ohata, N. Takai, H. Kagami, Spatial evaluation of tsunami refuge facilities in the central Kushiro city: simulation of evacuation behavior from tsunami utilizing multi agent system Part 2, *J. Architect. Plann., ALJ* 72 (612) (2007) 87–91 [in Japanese].
- [6] T. Takeuchi, A. Kondo, M. Yamaguchi, Y. Hamada, Empirical analysis on evaluation of refuge facilities from tsunami in consideration of the capacity; A case study in Susaki city-, infrastructure planning review, *Jpn. Soc. Civ. Eng.* 20 (2) (2003) 345–354 [in Japanese].
- [7] Y. Hamada, A. Kondo, K. Watanabe, T. Takeuchi, M. Yamaguchi, Planning of allocation of evacuation facilities based on residents awareness of disaster prevention, in: *A Case Study in Susaki City, Infrastructure Planning Review*, vol. 22, Japan Society of Civil Engineers, 2005, pp. 315–323 [in Japanese].
- [8] E. Ito, H. Kawase, S. Matsushima, M. Hatayama, Tsunami evacuation simulation considering road blockage by collapsed buildings evaluated from predicted strong ground motion, *Nat. Hazards* 101 (2020) 959–980, <https://doi.org/10.1007/s11069-020-03903-2>.
- [9] F. Ashar, D. Amaratunga, R. Haigh, The analysis of tsunami vertical shelter in Padang city, *Procedia Econom. Finan.* 18 (2014) 916–923.
- [10] A. Santos, N. Fonseca, M. Queirós, J.L. Zêzere, J.L. Bucho, Implementation of tsunami evacuation maps at setubal municipality, Portugal, *Geosciences* 7 (4) (2017) 116, <https://doi.org/10.3390/geosciences7040116>.
- [11] V.M. Cruz-Atienza, Y. Ito, V. Kostoglodov, V. Hjörleifsdóttir, A. Iglesias, J. Tago, M. Caló, J. Real, A. Husker, S. Ide, T. Nishimura, M. Shinohara, C. Mortera-Gutierrez, S. García, M. Kido, A seismogeodetic amphibious network in the Guerrero seismic gap, Mexico, *Seismol. Res. Lett.* 89 (4) (2018) 1435–1449, <https://doi.org/10.1785/0220170173>.
- [12] V. Kostoglodov, S.K. Singh, J.A. Santiago, S.I. Franco, K.M. Larson, A.R. Lowry, R. Bilham, A large silent earthquake in the Guerrero seismic gap, Mexico, *Geophys. Res. Lett.* 30 (15) (2003) 1–4.
- [13] T. Miyashita, N. Mori, K. Goda, Uncertainty of probabilistic tsunami hazard assessment of Zihuatanejo (Mexico) due to the representation of tsunami variability, *Coast Eng. J.* 62 (3) (2020) 413–428, <https://doi.org/10.1080/21664250.2020.1780676>.
- [14] G. Nakano, K. Yamori, T. Miyashita, L. Urra, E. Mas, S. Koshimura, Combination of school evacuation drill with tsunami inundation simulation: consensus-making between disaster experts and citizens on an evacuation strategy, *Int. J. Disaster Risk Reduct.* (2020) 101803, <https://doi.org/10.1016/j.ijdr.2020.101803>.
- [15] M. Hatayama, T. Kosaka, A. Hernández-Hernández, Analysis on tsunami evacuation options with agent-based simulation in tourist area, in: *2018 5th International Conference on Information and Communication Technologies for Disaster Management (ICT-DM)*, 2018.
- [16] F. Imamura, Review of tsunami simulation with a finite difference method, in: H. Yeh, P. Liu, C.E. Synolakis (Eds.), *Long-Wave Runup Models*, World Scientific Publishing Co, Singapore, 1996, pp. 25–42. <https://bit.ly/3lubVr9>. (Accessed 4 August 2021).
- [17] N. Mori, A. Muhammad, K. Goda, T. Yasuda, A. Ruiz-Angulo, Probabilistic tsunami hazard analysis of the pacific coast of Mexico: case study based on the 1995 colima earthquake tsunami, *Front. in Built Environ.* 3 (34) (2017) 1–16, <https://doi.org/10.3389/fbuil.2017.00034>.
- [18] Y. Okada, Internal deformation due to shear and tensile faults in a half space, *Bull. Seismol. Soc. Am.* 82 (2) (1992) 1018–1040. <https://pubs.geoscienceworld.org/ssa/bssa/article-abstract/82/2/1018/119580/internal-deformation-due-to-shear-and-tensile?redirectedFrom=fulltext>. (Accessed 4 August 2021).
- [19] M. Hatayama, Development of Space-Time Geographic Information Systems DiMSIS, GIS – Theory and Application, 7/2, 1999, pp. 25–33 [in Japanese].
- [20] T. Kameda, Introduction to Pedestrian Agent Simulation using Artiscoc: from Principle and Methodology to Space Design and Management for Safety and Crowd, Kozo Keikaku Engineering Inc., Shoseki Kobo Hayama Publishing, 2010 [in Japanese].
- [21] Instituto Nacional de Estadística y Geografía (INEGI), Cartografía Geoestadística Urbana y Rural Amanzanada, Junio 2016, 2016. <http://www3.inegi.org.mx/sistema/biblioteca/ficha.aspx?upc=702825218799>. (Accessed 4 August 2021).
- [22] Instituto Nacional de Estadística y Geografía (INEGI), Modelo digital de elevación de alta resolución Lidar 2008, accessed 27 October 2017, 2008.
- [23] Instituto Nacional de Estadística y Geografía (INEGI), Cartografía geoestadística urbana, Cierre de los Censos Económicos 2014, DENU, 2015. <https://datos.gob.mx/busca/dataset/cartografia-geoestadistica-urbana-cierre-de-los-censos-economicos-2014-denu-01-2015>. (Accessed 4 August 2021).
- [24] QGIS Development Team, QGIS geographic information system, Open Source Geospatial Foundation Project, <http://qgis.osgeo.org>, 2017.
- [25] Fire and Disaster Management Agency, Guideline for Tsunami Evacuation Plan Development in Municipalities, (Chapter 2), Report on the development of the manual for promoting the countermeasures for tsunami [in Japanese], 2002. [https://www.fdma.go.jp/singi\\_kento/kento/items/kento106\\_01\\_p00.pdf](https://www.fdma.go.jp/singi_kento/kento/items/kento106_01_p00.pdf).
- [26] Instituto Nacional de Estadística y Geografía (INEGI), Censo de Población y Vivienda 2010, accessed 4 August 2021, 2010. <https://www.inegi.org.mx/programas/ccpv/2010/>.
- [27] K. Kumagai, Validation of tsunami evacuation simulation to evacuation activity from the 2011 off the pacific coast of Tohoku earthquake tsunami, *J. Jpn. Soc. Civ. Eng. Ser. D3 (Infrastruct. Plann. Manag.)* 70 (5) (2014) I\_187–I\_196, 2014. (in Japanese with English abstract).
- [28] G. Bernardini, M. Postacchini, E. Quagliarini, M. Brocchini, C. Cianca, M. D’Orazio, A preliminary combined simulation tool for the risk assessment of pedestrians’ flood-induced evacuation, *Environ. Model. Software* 96 (2017) 14–29.
- [29] G. Bernardini, E. Quagliarini, M. D’Orazio, M. Brocchini, Towards the simulation of flood evacuation in urban scenarios: experiments to estimate human motion speed in floodwaters, *Saf. Sci.* 123 (2020) 104563, <https://doi.org/10.1016/j.ssci.2019.104563>.